# Where do slopes fail in Rudraprayag? A small-inventory landslide susceptibility study, and how evaluation choices change the answer

Gauri Makker

VIT Bhopal University, India
gaurimakker2006@gmail.com
ORCID: 0009-0008-4747-3151

This manuscript is a non-peer-reviewed preprint submitted to EarthArXiv. It has not been submitted to a journal for peer review.

# Where do slopes fail in Rudraprayag? A small-inventory landslide susceptibility study, and how evaluation choices change the answer

Gauri Makker
VIT Bhopal, India
gaurimakker2006@gmail.com
ORCID: 0009-0008-4747-3151

September 2026

**Abstract**

Rudraprayag district in the Garhwal Himalaya (Uttarakhand, India) is highly landslide-prone and lies on the pilgrimage route to Kedarnath. No landslide inventory was accessible for this study, so I built a preliminary one semi-automatically: bare, steep patches detected in Sentinel-2 imagery were verified one by one on high-resolution imagery, giving 38 landslides. I trained random forests on four terrain factors (elevation, slope, aspect and distance to river) and evaluated them with spatial cross-validation. Evaluation choices changed the results substantially. With background (non-landslide) points drawn across the whole district, a model that knew only each point's coordinates scored almost as well as the terrain model (AUC 0.83 vs 0.85). Adding vegetation and land cover raised the AUC to 0.93–0.95, but only because the landslides had been detected as bare ground. Results from any single random draw of background points were unreliable: across 20 draws, the same model's AUC ranged from 0.42 to 0.86. With background points matched within 3 km of each landslide and results reported across 20 random draws, the terrain model reaches a within-area AUC of 0.74 on average (95% of draws: 0.52–0.85) and beats a location-only model in 90% of draws. A map averaged over 20 models places 87% of held-out landslides (95% range 73–94%) in its two highest classes, which cover 40% of the area, compared with 49% of nearby stable slopes. Satellite rainfall (NASA GPM IMERG, 1998–2025) shows that the monsoon brings about 72% of annual rainfall, and that June 2013, the month of the Kedarnath disaster, was the wettest June on record, although 2013 was only the third wettest monsoon overall. The results are preliminary. The main contributions are an open inventory and pipeline, and a worked demonstration of how common sampling and evaluation choices can overstate the skill of small-inventory susceptibility models.

**Keywords:** landslide susceptibility; spatial cross-validation; random forest; background sampling; Himalaya; Sentinel-2; GPM IMERG

## 1 Introduction

Landslides are among the most damaging natural hazards in Uttarakhand. They block highways, cut off villages and cause deaths nearly every monsoon. In June 2013, extreme rainfall, together with the outburst of the moraine-dammed Chorabari Lake above Kedarnath, caused the Kedarnath disaster in Rudraprayag district, one of the deadliest hazard events in the Indian Himalaya (Dobhal et al., 2013). Knowing which slopes are most likely to fail helps decide where to monitor, reinforce, or warn.

Landslide susceptibility mapping estimates where landslides are likely, based on the conditions at locations where they have occurred before. Statistically based and machine-learning models are widely used for this (Reichenbach et al., 2018), and several studies have mapped Rudraprayag district with such methods (Saha et al., 2020, 2021), reporting high predictive performance.

Two methodological issues make such performance figures hard to interpret. First, landslide data are spatially clustered: when training and test points are close together, randomly split validation overstates how well a model predicts in new places, which is why spatial cross-validation is recommended (Brenning, 2005; Roberts et al., 2017; Ploton et al., 2020). Second, susceptibility models need “non-landslide” (background) points, and how these are sampled shapes what the model learns.

This study asks what a fully transparent pipeline, built only from free data and a self-built inventory, can honestly support in Rudraprayag, and how robust its results are. The official and public inventories I tried were not accessible at the time: the Geological Survey of India’s Bhukosh portal was not loading, and NASA’s landslide catalog (COOLR) services returned errors. So I built a preliminary inventory myself.

The contributions are:

1. an open, preliminary landslide inventory for Rudraprayag, including all 299 saved review decisions (landslide / not a landslide / unsure);
2. an evaluation sequence showing three distinct ways in which a small-inventory model can appear more skilful than it is;
3. a susceptibility map averaged over 20 models, with flags for model disagreement and extrapolation;
4. a rainfall analysis placing the inventory in its monsoon context;
5. reproducible notebooks and an interactive web map.

## 2 Study area

Rudraprayag is one of Uttarakhand’s 13 districts, in the Garhwal Himalaya (Figure 1). It rises from about 700 m in the southern valleys to about 7,000 m around the peaks near Kedarnath in the north. The district is drained by the Mandakini, which flows south from the Kedarnath area, and the Alaknanda; the two meet at Rudraprayag town. Slopes are steep (most between 25° and 45°), and the main roads, including the route to Kedarnath, run along the river valleys. Most rainfall arrives with the summer monsoon (Section 5.5). The modelled area, defined in Section 4.3, covers about 1,590 $km^2$.

## 3 Data

All data are freely available (Table 1). Processing was done in Google Earth Engine (Gorelick et al., 2017) and Python. All layers were resampled to a common 30 m grid in UTM zone 44N (EPSG:32644) and clipped to the district (Figure 2).

## 4 Methods

### 4.1 Landslide inventory

Landslide candidates were detected automatically as Sentinel-2 pixels (October–December 2025) with NDVI $< 0.2$ and slope $> 25°$, below 3,500 m, and not classed as snow/ice or water in WorldCover. This candidate composite is separate from the NDVI layer in Table 1 (October 2024–March 2025), which was built earlier for the feature stack and is used only in the comparison model. The candidate composite covers the period just after the 2025 monsoon, so it also includes scars formed during that monsoon. Candidate pixels were grouped into patches, and patches of 0.2–20 ha were kept, giving 330 candidate patches. A random sample of 300 candidates was

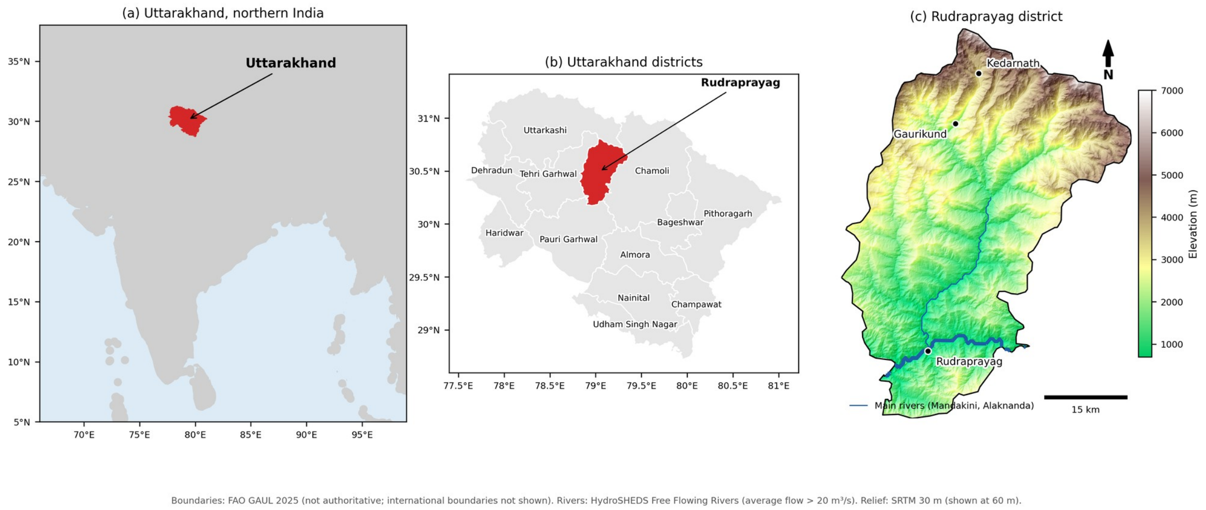


**Figure 1:** Study area. (a) Uttarakhand in northern India. (b) Uttarakhand's districts, with Rudraprayag highlighted. (c) Rudraprayag district: shaded relief coloured by elevation (SRTM), main rivers (HydroSHEDS, mean flow $>20\,\mathrm{m^3\,s^{-1}}$; line width proportional to flow) and key places. Boundaries are from FAO GAUL 2025 and are not authoritative; international boundaries are not shown.

**Table 1:** Data used in this study.

| Layer | Source | Use |
|---|---|---|
| Elevation, slope, aspect | SRTM 30 m (Farr et al., 2007) | Model features |
| NDVI | Sentinel-2 surface reflectance, median of Oct 2024–Mar 2025 scenes with <20% cloud; $(B8 - B4)/(B8 + B4)$ (Rouse et al., 1974); built for the feature stack before the inventory | Comparison model only |
| Land cover | ESA WorldCover 10 m v200 (Zanaga et al., 2022) | Comparison model only; masking |
| Distance to river | HydroSHEDS Free Flowing Rivers (Grill et al., 2019) | Model feature |
| District boundary | FAO GAUL 2025 (FAO, 2025) | Study area |
| Landslide candidates | Sentinel-2 NDVI composite, Oct–Dec 2025 (after the 2025 monsoon); a separate composite from the NDVI layer above | Inventory |
| Rainfall | NASA GPM IMERG V07, monthly, 0.1° (∼11 km), 1998–2025 (Huffman et al., 2019) | Rainfall analysis |

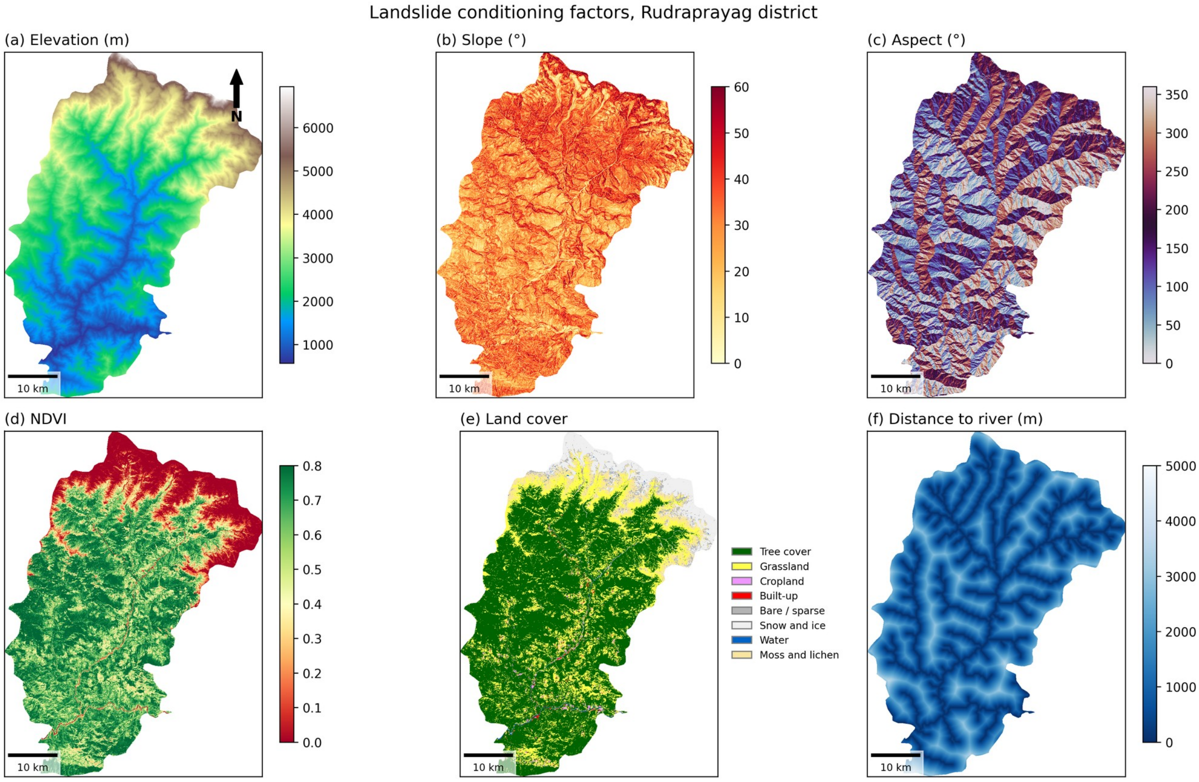


**Figure 2:** The six conditioning factors: elevation, slope, aspect, NDVI, land cover (ESA WorldCover classes) and distance to river.

reviewed one by one at high zoom on Google satellite imagery, in a custom Earth Engine review tool, and labelled landslide, not a landslide, or unsure.

The review followed fixed rules. Stream beds, gullies, riverbeds, roads, buildings, construction sites and shadowed cliffs were labelled "not a landslide". Bright, clean bare patches cut into vegetation with sharp edges spreading downhill, streamside slides, and debris fans fed by steep channels were labelled "landslide". Ambiguous cases were labelled "unsure", as was any candidate still undecided after about 30 seconds. Landslide points (patch centres) within 200 m of each other were merged to remove duplicates.

## 4.2 Background (stable) points

A susceptibility model compares landslide locations with locations assumed to be stable. I used three sampling designs, each with one stable point per landslide (38 each):

- **Naive:** random pixels anywhere in the same terrain as the candidates (below 3,500 m, not snow/ice or water), at least 500 m from any landslide.
- **Matched:** for each landslide, one random pixel within 3 km, in the same terrain and at least 500 m from any landslide. This removes regional differences, so the model has to answer a local question: why did this slope fail, and not a similar slope in the same valley?
- **Matched + slope $> 25°$:** as matched, but also requiring a slope above 25°, the same rule the landslide candidates had to pass. This tests whether the candidate filter itself creates an apparent slope signal.

### 4.3 Features and model

The main model uses four terrain features that describe a slope before it fails: elevation, slope, aspect (converted to sine and cosine, because aspect is circular) and distance to river. NDVI and land cover were *excluded* from the main model. The landslides were found by searching for bare ground (NDVI $< 0.2$), and WorldCover maps fresh scars as bare, so these features largely describe the scar itself rather than the conditions before failure. A comparison model including them was run to measure this effect.

Models are random forests (Breiman, 2001) in scikit-learn (Pedregosa et al., 2011), with 300 trees and at least 2 samples per leaf for evaluation. The modelled domain is the same as the sampling domain: pixels below 3,500 m that are not snow/ice or water.

### 4.4 Evaluation

Performance is measured with the area under the ROC curve (AUC): the probability that the model scores a randomly chosen landslide above a randomly chosen stable point (Hanley and McNeil, 1982). An AUC of 0.5 is chance.

**Spatial cross-validation.** Points were grouped into five geographic blocks with k-means clustering on their coordinates. Each block was held out in turn while the model was trained on the other four. I report two versions:

- **Pooled AUC:** predictions from all held-out blocks combined into one AUC.
- **Within-block AUC:** AUC computed inside each held-out block (where it contains both classes), then averaged. This matches the question of whether the model can separate a failing slope from stable slopes in the same area.

**Location baseline.** A model using only the $x$ and $y$ coordinates shows how much can be achieved just by knowing where a point is. A terrain model that barely beats it has mostly learned geography.

**Across draws.** With only 38 stable points, the particular random draw matters. For the matched designs I therefore repeated the whole procedure for 20 independent draws of stable points (with a new block layout each time), and report the mean and the range containing 95% of draws.

### 4.5 Susceptibility map and held-out check

The final map averages 20 random forests (100 trees each), one per draw of stable points in the matched design. Each model scores every pixel in the modelled domain. Because the model is trained on equal numbers of landslide and stable points, scores are relative, not probabilities, so the map is shown as five classes that each cover 20% of the modelled area (quintiles). The standard deviation of the 20 scores at each pixel measures model disagreement. Pixels more than 5 km from any training point are flagged as extrapolation.

To check the map against landslides it has not seen, I repeated the mapping without each of five areas (k-means blocks based on the landslides only). For each area, 20 models trained without it were averaged, and I recorded which class (by that model's own quintiles) each held-out landslide and held-out stable point fell in. If the map had no skill, about 40% of landslides would fall in the top two classes by chance. The 95% range for the landslide share uses the Wilson interval (Wilson, 1927).

### 4.6 Rainfall

District-average monthly rainfall was taken from IMERG V07 (monthly mean rate $\times$ hours in the month) for January 1998 to September 2025. I computed monsoon (June–September) totals for each year with all four months available. A map of mean monsoon rainfall (1998–2025) was compared with the susceptibility classes. Because the inventory has no failure dates, rainfall could not be linked to individual landslides. Because IMERG pixels ($\sim$11 km) are much larger than the distance between each landslide and its stable point ($\leq$ 3 km), rainfall was not used as a model feature.

### 4.7 Reproducibility

All random steps use fixed seeds; re-running the full pipeline after a session restart reproduced every reported number exactly. Notebooks, data and figures are available in the repository (see Data and code availability).

## 5 Results

### 5.1 Inventory

Of the 300 reviewed candidates, 42 were landslides, 190 were not, and 68 were unsure; the last decision (an "unsure") was lost before saving, so the published file contains 299 decisions (42, 190 and 67). About 18% of the decided candidates (42 of 232) were landslides. Most false candidates were riverbeds, stream channels and road cuts. After merging duplicates, the inventory contains **38 landslides** (Figure 3). They cluster in the north, especially the upper Mandakini valley along the Kedarnath route, while more of the area below 3,500 m lies in the south.

### 5.2 Naive sampling: learning where, not why

With naive background points, the terrain model reached a pooled spatial-CV AUC of 0.85 (random CV: 0.84). But the coordinates-only model reached 0.83 (random CV: 0.79). Because landslides cluster in the north, "north" alone was almost as informative as all the terrain features (Figure 4a). Spatial CV scored no lower than random CV (0.852 $\pm$ 0.004 vs 0.841 $\pm$ 0.017 across 10 repeats), although it normally should, because it tests prediction in new places. The reason is that the blocks differed strongly in their landslide share, so the pooled AUC rewarded separating regions rather than slopes. Adding NDVI and land cover raised the AUC to 0.93–0.95 in both the naive and matched designs, confirming the circularity described in Section 4.3.

### 5.3 Matched sampling across 20 draws

With matched background points, the location shortcut largely disappears. Table 2 summarises the within-block AUC across 20 draws (Figure 4b).

**Table 2:** Within-block AUC across 20 random draws of stable points: mean (range containing 95% of draws).

| Features | Matched | Matched + slope > 25° |
|---|---|---|
| All terrain | 0.74 (0.52–0.85) | 0.69 (0.47–0.86) |
| Distance to river only | 0.64 (0.45–0.85) | 0.63 (0.44–0.79) |
| Aspect only | 0.64 (0.47–0.78) | 0.59 (0.37–0.78) |
| Elevation only | 0.54 (0.33–0.73) | 0.57 (0.38–0.73) |
| Slope only | 0.54 (0.40–0.74) | 0.48 (0.32–0.69) |
| Coordinates only | 0.59 (0.49–0.69) | 0.53 (0.39–0.64) |
| Terrain beats coordinates (share of draws) | 90% | 90% |

Four results stand out:

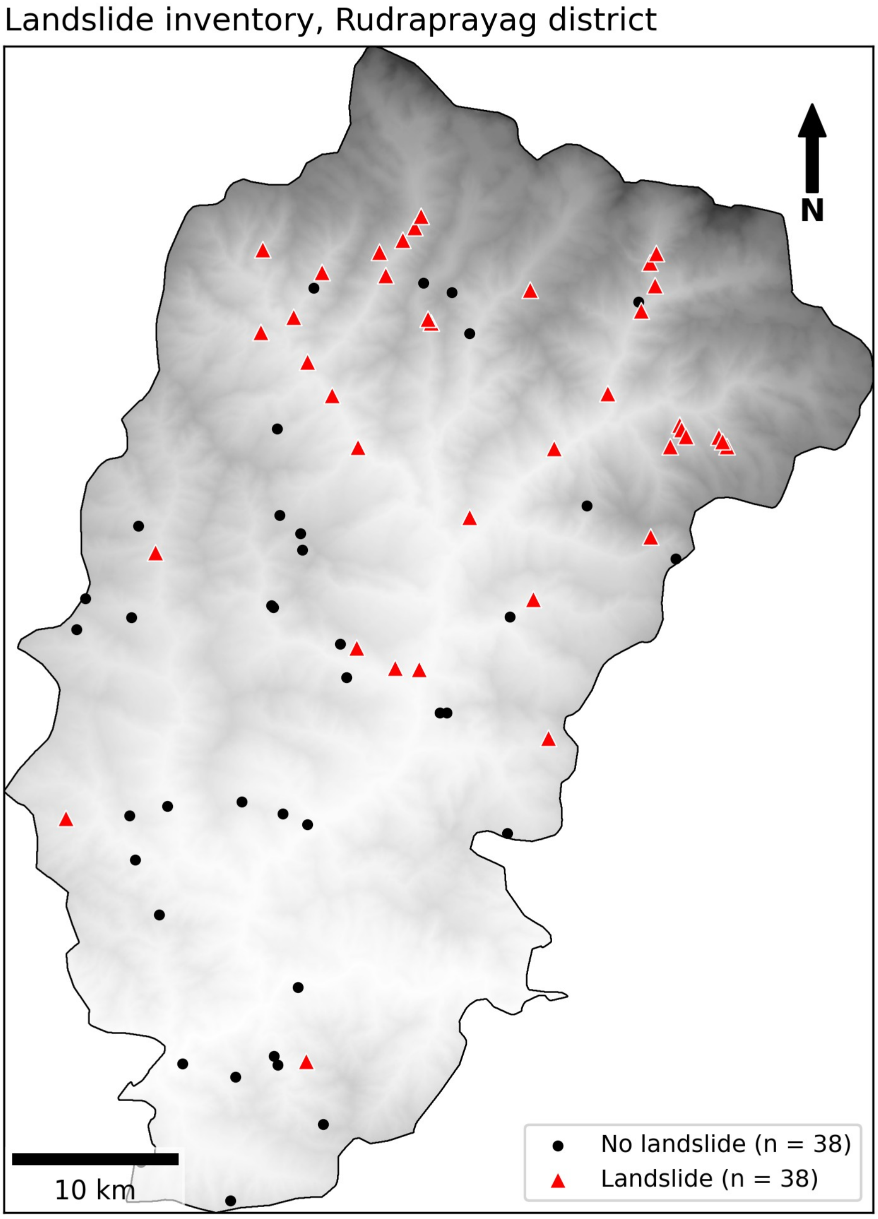


**Figure 3:** Preliminary landslide inventory: 38 verified landslides (red) and 38 naive background points (black) on elevation (darker = higher).

- **The terrain model has real, moderate skill.** It averages 0.74 and beats the location-only model in 90% of draws, by 0.16 on average, in both designs. Some location information remains even within areas (coordinates-only averages 0.59), but terrain adds clearly to it.
- **The candidate filter does not change the overall result much.** Requiring stable points to be steeper than 25° lowers the mean by about 0.05, and the ranges overlap almost completely.
- **Slope alone is close to chance.** In the matched design, the median slope of landslides and stable points is almost identical (36.9° vs 36.7°). The apparent slope signal in single draws came from the gentle tail: 10% of stable points were below 19.8°, while landslide candidates could not be below 25° by design. Once stable points follow the same rule, slope alone averages 0.48.
- **No single feature dominates.** Distance to river and aspect each carry a modest signal (about 0.6). The terrain model outperforms each single feature, so the features complement each other.

Single draws were misleading throughout. Across the 20 draws, the terrain model's within-block AUC ranged from 0.42 to 0.86 in the matched design. The single draw used initially (the same draw as in Figure 4a) suggested that slope carried a clear signal (0.66) and put aspect below chance (0.42). Neither held up across 20 draws.

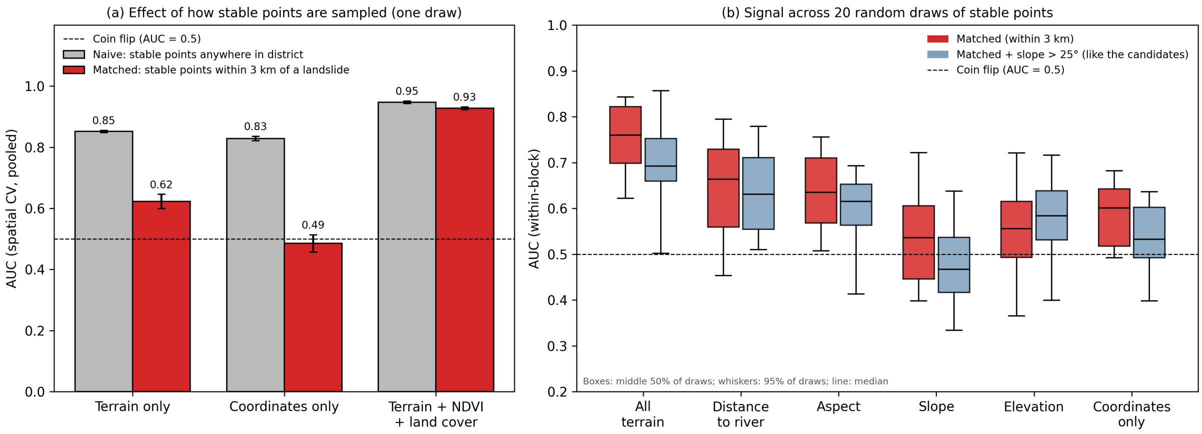


**Figure 4:** Model evaluation. (a) Pooled spatial-CV AUC for one draw of naive vs matched background points: with naive sampling, a coordinates-only model nearly matches the terrain model. Error bars show the standard deviation across 10 repeats with different random-forest seeds and block layouts; they do not include variation between draws of stable points, which is much larger (panel b). (b) Within-block AUC across 20 random draws of stable points, for the matched design and the matched design with slope > 25°. Boxes show the middle 50% of draws, whiskers extend to the most extreme draws within the 2.5th–97.5th percentiles, and lines the median. Note that the y-axis of (b) starts at 0.2.

## 5.4 Susceptibility map

The averaged map (Figure 5) shows the highest classes along the river network, particularly on the valley walls of the Mandakini, the Alaknanda and their tributaries, while ridges score low. The class breaks are 0.193, 0.285, 0.383 and 0.538.

**Robustness.** Compared with a map from a single model, the averaged map has a correlation of 0.90. 95% of pixels stay within one class, but only 60% stay in exactly the same class. The classes are therefore best read as broad bands. Model disagreement (mean standard deviation 0.088 on the 0–1 score) is highest along the rivers: the models agree that valley sides are riskier, but differ in how much riskier.

**Held-out check.** Of the held-out landslides, **87%** fell in the High or Very high class (33 of 38; 95% range 73–94%), and 61% in Very high alone. Of the held-out stable points (pooled across 20 draws), 49% fell in High or Very high and 23% in Very high. The chance levels are 40% and 20%. The map therefore separates failing slopes from their neighbours, not just risky valleys from safe ones. Stable points still fall slightly above chance, as expected, since they were drawn in the same valleys.

**Extrapolation.** 38.3% of the modelled area, mostly in the south, lies more than 5 km from any training point. Southern scores sit close to the class breaks, so the mixed classes there should not be read closely.

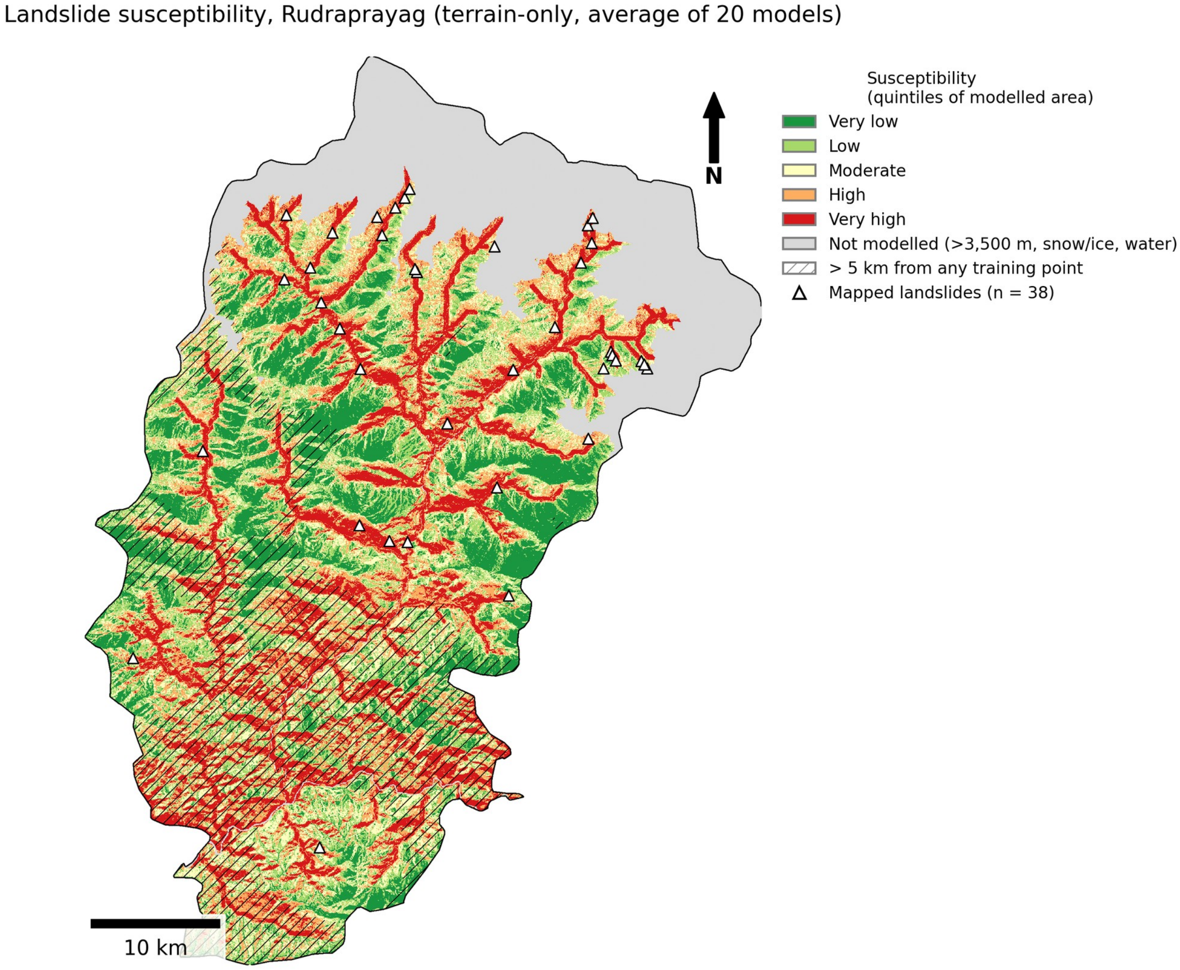


**Figure 5:** Landslide susceptibility, average of 20 terrain-only models. Classes are quintiles of the modelled area. Grey: not modelled (above 3,500 m, snow/ice, water). Hatched: more than 5 km from any training point. Triangles: the 38 mapped landslides (training data).

## 5.5 Rainfall

June–September brings an average of 1,336 mm, about 72% of the annual total of 1,865 mm, peaking in July and August (Figure 6). **June 2013 was the wettest June in the record**, with 501 mm against an average June of 176 mm, matching the rainfall behind the Kedarnath disaster. Yet **2013 was only the third wettest monsoon**, behind 2010 (1,924 mm, +44%) and 2011 (1,788 mm). The driest monsoon was 2009 (813 mm, −39%). The inventory was mapped after three above-average monsoons: 2023 (+5%), 2024 (+17%) and 2025 (+24%, the fourth wettest).

Across the district, mean monsoon rainfall ranges from about 940 mm in the southwest to about 1,660 mm in the northwest. It is essentially unrelated to susceptibility: mean rainfall differs by only about 3.5% between classes (1,322–1,368 mm), and exactly 33% of the Very high area lies in the wettest third of the district, the value expected with no relationship. At the points, 26 of 38 landslides share exactly the same rainfall value as their nearest stable point.

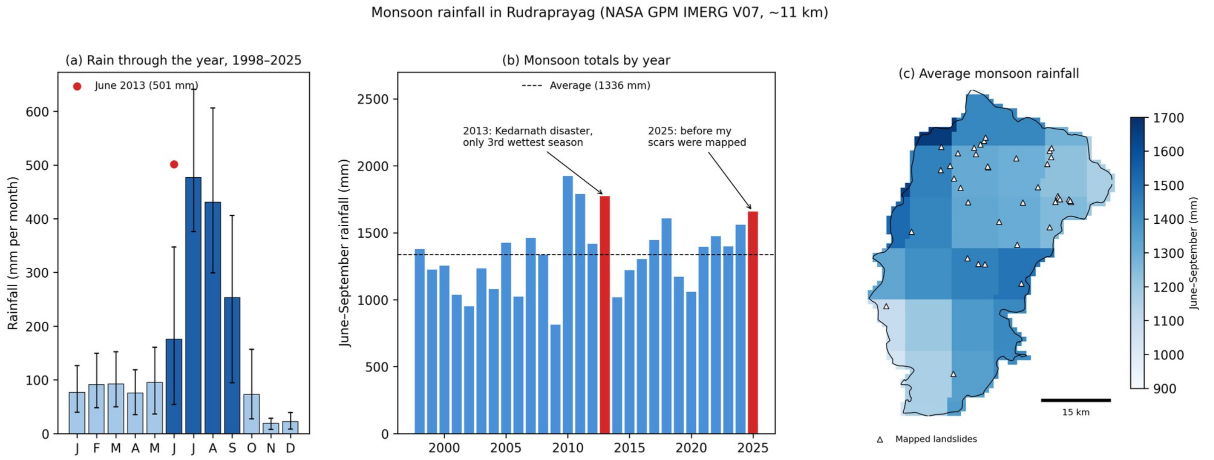


**Figure 6:** Monsoon rainfall in Rudraprayag (NASA GPM IMERG V07). (a) Mean rainfall per month, 1998–2025, with the 10th–90th percentile range across years; June 2013 in red. (b) June–September totals per year, with 2013 and 2025 highlighted. (c) Mean monsoon rainfall (∼11 km data shown at 1 km) with the mapped landslides.

# 6 Discussion

## 6.1 What the model learned

Across all checks, the model's skill comes from identifying hazardous *valley sides*: slopes near rivers, with some contribution from aspect. River undercutting of slope toes is a plausible physical mechanism. However, in Rudraprayag the main roads also follow the rivers, and road cutting is a well-known landslide trigger. Without a road layer, this study cannot separate "near a river" from "near a road". The review rules also counted streamside slides as landslides, which may have strengthened the river signal. The aspect effect is plausible, because slope orientation affects sunlight, moisture and vegetation, but its range across draws is wide, so it should be treated as modest.

## 6.2 Three ways a small-inventory study can overstate skill

This study encountered three separate sources of inflated performance, each of which would have been easy to miss:

1. **Location shortcuts.** When landslides cluster regionally and background points are spread across the whole area, a model can score highly just by learning where landslides are. A coordinates-only baseline exposes this.

2. **Circular features.** Features used to find the landslides (here, low NDVI and, to a lesser extent, steep slopes) or features that describe the scar itself (bare land cover) inflate performance. Adding NDVI and land cover raised the pooled AUC from 0.85 to 0.95 with naive sampling, and from 0.62 to 0.93 with matched sampling.

3. **A single background draw.** With a small inventory, one random draw of background points can be misleading: across 20 draws, the same model's AUC ranged from 0.42 to 0.86,

and single draws even reversed conclusions about individual features. Reporting results across many draws is essential.

## 6.3 Comparison with published studies

Previous studies of Rudraprayag report higher performance. Saha et al. (2021) used 220 landslide locations from field surveys and records, twelve conditioning factors and four-fold cross-validation, and reported an AUC of about 0.89 for their best (ensemble) model. Saha et al. (2020) used sixteen conditioning factors with a random 70:30 split. These numbers are not directly comparable with mine. Those studies used much larger, field-based inventories and more conditioning factors. They also validated on randomly partitioned data, whereas this study uses spatially held-out areas, matched background points and only four terrain features, which is a deliberately harder test. A lower AUC here therefore does not mean that those results are wrong. It does suggest that performance figures depend strongly on the sampling and validation design, and that such designs should be reported alongside the numbers.

## 6.4 Rainfall

The rainfall analysis supports a familiar point: seasonal totals do not tell you when slopes fail. The 2013 disaster came from a short, extreme burst within a monsoon that was not the wettest overall. Short-duration rainfall (hours to days) is therefore more relevant for early warning than seasonal totals. The independence of monsoon rainfall and terrain susceptibility means that the two carry separate information: a slope's overall hazard depends on both. The inventory was mapped after three above-average monsoons, which is consistent with the many fresh scars found, but without failure dates this cannot be tested.

## 6.5 Limitations

- **Small inventory:** 38 landslides from a single interpreter, with no field verification. Ranges across draws are correspondingly wide.
- **Detection bias:** only landslides still bare in late 2025 and larger than 0.2 ha could be found. Old, revegetated or small landslides are missing, and bare scars may be easier to spot in some terrain than others.
- **Points, not polygons:** each landslide is represented by the centre of its bare patch, not its initiation point.
- **Missing factors:** lithology, faults, soil and roads were not included. They are important in many published models, and roads in particular may be confounded with distance to river here.
- **Extrapolation:** 38% of the map is more than 5 km from any training point.
- **Rainfall resolution:** IMERG's $\sim$11 km pixels are too coarse for slope-scale analysis, and satellite rainfall in steep mountains is uncertain. The June 2013 check is reassuring but is not a validation against rain gauges.
- **Boundaries:** administrative boundaries are from FAO GAUL and are not authoritative.

## 6.6 Future work

The most valuable next step is a larger and independent inventory: reviewing the remaining candidates, loosening the candidate filter, and above all validating against official records, for example from the Geological Survey of India or the Uttarakhand Landslide Mitigation and

Management Centre, if they can be obtained. Adding road, lithology and fault layers would test the river–road confound. Daily or sub-daily rainfall combined with dated landslide records would allow the timing of failures to be studied properly.

# 7 Conclusions

- A transparent, free-data pipeline with a self-built inventory of 38 landslides can identify hazardous valley sides in Rudraprayag with moderate skill: a within-area AUC of 0.74 on average (95% of draws 0.52–0.85), beating a location-only model in 90% of draws.
- The averaged map places 87% of held-out landslides in its top two classes (chance: 40%), compared with 49% of nearby stable slopes.
- Three common choices (district-wide background sampling, circular features and single background draws) each inflate or distort performance. With small inventories, location baselines and repeated background draws should be standard.
- The monsoon brings about 72% of annual rainfall, but seasonal totals do not identify disaster years: 2013 had the wettest June on record, yet only the third wettest monsoon.
- All results are preliminary. The map is not an official hazard map and should not be used for safety or planning decisions.

# Data and code availability

All notebooks, data (inventory, review decisions, training points, rainfall series, AUCs across draws) and figures are available at `https://github.com/makkergauri/uttarakhand-landslide-risk`. The interactive map is at `https://makkergauri.github.io/uttarakhand-landslide-risk/`.

# Acknowledgements

I thank the providers of the free datasets used here: NASA (SRTM, GPM IMERG), ESA and the Copernicus programme (Sentinel-2, WorldCover), WWF (HydroSHEDS), FAO (GAUL) and Google Earth Engine. This work contains modified Copernicus Sentinel data (2024–2025).

# Declarations

**Funding.** This work received no funding.
**Competing interests.** The author declares no competing interests.

# References

Breiman, L. (2001). Random forests. *Machine Learning*, 45(1), 5–32. `https://doi.org/10.1023/A:1010933404324`

Brenning, A. (2005). Spatial prediction models for landslide hazards: review, comparison and evaluation. *Natural Hazards and Earth System Sciences*, 5(6), 853–862. `https://doi.org/10.5194/nhess-5-853-2005`

Dobhal, D. P., Gupta, A. K., Mehta, M., & Khandelwal, D. D. (2013). Kedarnath disaster: facts and plausible causes. *Current Science*, 105(2), 171–174.

FAO (2025). Global Administrative Unit Layers (GAUL) 2025. Food and Agriculture Organization of the United Nations.

Farr, T. G., et al. (2007). The Shuttle Radar Topography Mission. *Reviews of Geophysics*, 45, RG2004. https://doi.org/10.1029/2005RG000183

Gorelick, N., Hancher, M., Dixon, M., Ilyushchenko, S., Thau, D., & Moore, R. (2017). Google Earth Engine: planetary-scale geospatial analysis for everyone. *Remote Sensing of Environment*, 202, 18–27. https://doi.org/10.1016/j.rse.2017.06.031

Grill, G., et al. (2019). Mapping the world's free-flowing rivers. *Nature*, 569, 215–221. https://doi.org/10.1038/s41586-019-1111-9

Hanley, J. A., & McNeil, B. J. (1982). The meaning and use of the area under a receiver operating characteristic (ROC) curve. *Radiology*, 143(1), 29–36. https://doi.org/10.1148/radiology.143.1.7063747

Huffman, G. J., Stocker, E. F., Bolvin, D. T., Nelkin, E. J., & Tan, J. (2019). GPM IMERG Final Precipitation L3 1 month 0.1 degree × 0.1 degree V07. Goddard Earth Sciences Data and Information Services Center (GES DISC). https://doi.org/10.5067/GPM/IMERG/3B-MONTH/07

Pedregosa, F., et al. (2011). Scikit-learn: machine learning in Python. *Journal of Machine Learning Research*, 12, 2825–2830.

Ploton, P., et al. (2020). Spatial validation reveals poor predictive performance of large-scale ecological mapping models. *Nature Communications*, 11, 4540. https://doi.org/10.1038/s41467-020-18321-y

Reichenbach, P., Rossi, M., Malamud, B. D., Mihir, M., & Guzzetti, F. (2018). A review of statistically-based landslide susceptibility models. *Earth-Science Reviews*, 180, 60–91. https://doi.org/10.1016/j.earscirev.2018.03.001

Roberts, D. R., et al. (2017). Cross-validation strategies for data with temporal, spatial, hierarchical, or phylogenetic structure. *Ecography*, 40(8), 913–929. https://doi.org/10.1111/ecog.02881

Rouse, J. W., Haas, R. H., Schell, J. A., & Deering, D. W. (1974). Monitoring vegetation systems in the Great Plains with ERTS. *Third Earth Resources Technology Satellite-1 Symposium*, NASA SP-351, 309–317.

Saha, S., Saha, A., Hembram, T. K., Pradhan, B., & Alamri, A. M. (2020). Evaluating the performance of individual and novel ensemble of machine learning and statistical models for landslide susceptibility assessment at Rudraprayag district of Garhwal Himalaya. *Applied Sciences*, 10(11), 3772. https://doi.org/10.3390/app10113772

Saha, S., Arabameri, A., Saha, A., Blaschke, T., Ngo, P. T. T., Nhu, V. H., & Band, S. S. (2021). Prediction of landslide susceptibility in Rudraprayag, India using novel ensemble of conditional probability and boosted regression tree-based on cross-validation method. *Science of the Total Environment*, 764, 142928. https://doi.org/10.1016/j.scitotenv.2020.142928

Wilson, E. B. (1927). Probable inference, the law of succession, and statistical inference. *Journal of the American Statistical Association*, 22(158), 209–212. https://doi.org/10.1080/01621459.1927.10502953

Zanaga, D., et al. (2022). ESA WorldCover 10 m 2021 v200. https://doi.org/10.5281/zenodo.7254221